DR. KELLY J HUFFMAN (Orcid ID : 0000-0003-4918-4413)

Article type : Original Research Article

TITLE: The impact of paternal alcohol consumption on offspring brain and behavioral development.

AUTHORS: Kathleen E. Conner[1]*, BS, BA; Riley T. Bottom[1]*, BS; Kelly J. Huffman[1,2], PhD
*These authors contributed equally to this work.

AFFILIATIONS: 1- Interdepartmental Neuroscience Program, University of California, Riverside
2- Department of Psychology, University of California, Riverside

CORRESPONDENCE ADDRESS:
Kelly J. Huffman, PhD
Department of Psychology, University of California, Riverside, 900 University Avenue, Riverside, CA 92521
Tel.: 951-827-4805
Fax: 951-827-3985
E-mail: kelly.huffman@ ucr.edu

Key Words: Paternal ethanol exposure, Brain development, Neocortex, Behavior, Neuroanatomy

This article has been accepted for publication and undergone full peer review but has not been through the copyediting, typesetting, pagination and proofreading process, which may lead to differences between this version and the Version of Record. Please cite this article as doi: 10.1111/ACER.14245

ABSTRACT

Background: Fetal alcohol spectrum disorders (FASD) describe the wide array of long-lasting developmental abnormalities in offspring due to prenatal alcohol (ethanol, EtOH) exposure via maternal gestational drinking. Although the teratogenic consequences of prenatal ethanol exposure, or PrEE, are apparent, the effects of preconception paternal ethanol exposure (PatEE) are still unclear. Previous research suggests that PatEE can induce molecular changes and abnormal behavior in the offspring. However, it is not known if PatEE impacts the development of the neocortex and behavior in offspring as demonstrated in maternal consumption models of FASD (El Shawa et al., 2013). **Methods:** In this study, we utilized a novel mouse model of PatEE where male mice self-administered 25% EtOH for an extended period prior to conception, generating indirect exposure to the offspring through the paternal germline. Following mating, we examined the effects of PatEE on offspring neocortical development at postnatal day (P) 0 and evaluated several aspects of behavior at both P20 and P30 using a battery of behavioral assays. **Results:** PatEE resulted in significant impact on neocortical development, including abnormal patterns of gene expression within the neocortex at P0, as well as subtle alterations in patterns of intraneocortical connections. Additionally, PatEE mice exhibited a sex-specific increase in activity and sensorimotor integration deficits at P20, as well as decreased balance, coordination, and short-term motor learning at P30. This suggests that PatEE may generate long-lasting, sex-specific effects on offspring behavior. **Conclusions:** These results demonstrate that the developmental impact of preconception PatEE is more harmful than previously thought and provide additional insights into the biological mechanisms that may underlie atypical behavior observed in children of alcoholic fathers.

INTRODUCTION

In humans, prenatal ethanol exposure (PrEE) can result in fetal alcohol spectrum disorders, or FASD. This designation incorporates a variety of long-lasting cognitive and behavioral deficits (Hoyme et al., 2016) and has incidence rates as high as 5% in the United States (May et al., 2018). Much less is known about the impact of preconception paternal ethanol exposure (PatEE), despite a growing body of preclinical evidence indicating that offspring sired by males exposed to ethanol (EtOH) prior to conception display altered brain and behavioral development similar to maternally-mediated prenatal EtOH exposure (Jamerson et al., 2004; Meek et al., 2007; Kim et al., 2014; Finegersh and Homanics, 2014; Rompala et al., 2016; 2017; Chang et al., 2017; 2019). Additionally, clinical research in humans has found associations among heavy paternal EtOH consumption and adverse developmental outcomes in offspring (reviewed in Finegersh et al., 2015; Zuccolo et al., 2017; Xia et al., 2018), providing further support for the deleterious impact of paternal drinking. Although research investigating the impact of PatEE is on the rise, it remains greatly understudied compared to models of FASD generated from EtOH exposure via maternal drinking.

The neocortex, the largest part of the human brain, has many emergent properties that mediate complex, higher-order functions and behaviors. The neocortex relies on a tightly regulated temporal and spatial orchestration of genetic and environmental cues for proper development, a process that seems particularly susceptible to prenatal EtOH insult. Animal studies focusing on maternal EtOH exposure have found a plethora of atypical cortical phenotypes present in offspring including increased apoptosis (Ikonomidou et al., 2000), altered pyramidal cell morphology (Granato et al., 2003), modified development of anatomical regions or structures (Abbott et al., 2016) and atypical development of the intra-neocortical circuitry (El Shawa et al., 2013). Human neuroimaging studies in children with FASD have also demonstrated abnormalities in neocortical development (Zhou et al., 2011), suggesting that irregular cortical phenotypes may underlie some PrEE-induced behavioral alterations.

One particular aspect of neocortical development affected by prenatal EtOH exposure is arealization, or the patterning of neurons into functionally and spatially distinct areas

(Krubitzer and Huffman, 2000). Specifically, prenatal EtOH exposure results in aberrant intraneocortical connections (INCs), as well as altered expression of genes critical for proper patterning of the neocortex in mice (El Shawa et al., 2013). Recently, we have demonstrated that these phenotypes pass to second and third filial generations after an initial prenatal EtOH exposure (Abbott et al., 2018), suggesting EtOH may have potent transgenerational effects. Despite a growing body of research on how PrEE impacts the neocortex, there is a paucity of data regarding how paternal ethanol exposure may alter cortical development.

Preclinical studies focusing on PatEE's effects on the neocortex are sparse but have shown that affected offspring have increased cortical thickness (Jamerson et al., 2004) as well as altered expression and epigenetic regulation of the dopamine transporter in frontal cortex (Kim et al., 2014). Importantly, to our knowledge, no study exists examining the effect of preconception paternal EtOH consumption on development of neocortical connections. Due to the ability of PatEE to disrupt normal development in the neocortex, as well as EtOH's particular ability to modify INCs in absence of direct exposure, we hypothesized that PatEE offspring could also demonstrate abnormal neocortical development.

The goal of this study was to characterize the impact of a paternal binge of EtOH prior to conception on offspring cortical development. Specifically, we analyzed neocortical thickness, gene expression, and development of INCs in newborn mice. We also examined behavioral effects of PatEE in pre- and peri-pubescent mice at ages P20 and P30 using a battery of assays. Results from this study suggest that the paternal environment before conception is critical for healthy offspring development.

MATERIALS AND METHODS

Animal care.

All studies were conducted under research protocol guidelines approved by the Institutional Animal Care and Use Committee (IACUC) at UCR. CD-1 mice were initially purchased from Charles River Laboratories (Wilmington, MA/USA). All subjects were housed in UCR animal facilities under a standard 12h/12h light/dark cycle. All efforts were made to minimize animal discomfort and the number of mice utilized.

Ethanol administration and breeding.

Male mice, aged 3-6 months, were separated into control and EtOH exposed groups. Initially, experimental EtOH-treated male mice (n = 10) were provided a 25% EtOH-in-water solution, *ad libitum,* for 15 days as well as standard mouse chow (Fig.1). Control males (n = 10) were provided *ad libitum* water and standard mouse chow. After the binge period, P90 female mice were paired with control or EtOH-treated sires at the beginning of the dark cycle for breeding. The day of conception was determined by presence of vaginal plug, after which males were removed from the dam's cage. If no vaginal plug was observed, the male was returned to his home cage for continued treatment of EtOH or water for the remainder of the day and then placed back into the breeding cage at the start of the dark cycle. The average time to conception was 3.5 days for EtOH sires and 2.8 days for control sires. Each group had a time-to-conception of 0-8 days with total length of treatment being 15-23 days. All pregnant female mice were housed individually and provided standard mouse chow and water *ad libitum*. All female dams were EtOH-naïve and did not have access to EtOH.

Sire daily intake and blood ethanol content measurements.

Daily measurements of food and liquid intake of male mice were recorded at 1200 h to assess confounding nutritional differences between experimental and control groups. Each male was provided 100g of food and the chow was re-weighed daily at noon and replenished to 100g. Daily liquid intake (25% EtOH-in-water or water alone) for sires was measured using a graduated drinking bottle. Average daily values for food and liquid intake of experimental mice as well as weight gain were compared to control mice using *t*-test analyses. Also, body weights, in grams, were recorded for all mice at the beginning of exposure, when the ethanol solution was provided and at the end when ethanol was removed, to eliminate weight gain differences as a potential confound. Blood ethanol concentration (BEC) of a separate subset of males, resulting from treatment of 25% EtOH in water (n = 7) or water alone (n = 7), was determined using an alcohol dehydrogenase-based enzymatic assay (Pointe Scientific, Canton, MI/USA; see Supplemental Methods for details).

Pup measurement and tissue preparation.

On the day of birth, P0, the litter sizes were recorded. Pups born to dams bred with EtOH-treated sires were designated as PatEE pups and pups born to dams bred with water-treated sires were designated as controls. For each litter (n = 10, both groups), subsets of offspring were randomly designated for P0 analyses, P20 behavioral assessment, or P30 behavioral assessment in an effort to reduce potential litter effects and ensure an even sampling for each experimental endpoint. Experimental/control subsets per litter were limited to 2 ± 2 pups for P0 endpoints, 5 ± 2 pups for P20 endpoints, and 6 ± 2 pups for P30 endpoints, dependent on total litter size. Larger subsets were reserved for P20 and P30 behavioral assessment due to the statistical power needed for accurate sex-specific analysis; all efforts were made to limit 3 animals/per sex/per litter for each experimental endpoint. P0 pups used for dye tracing, anatomy, and gene expression studies were weighed, sacrificed via hypothermia and exsanguination, and transcardially perfused with 4% paraformaldehyde (PFA) in 0.1M phosphate buffer, pH 7.4. Due to the absence of distinguishing sexual characteristics at P0, the relative inaccuracy of using anogenital distances at this age (Greenham and Greenham, 1977), and the absence of pigment in albino CD-1 mice (Wolterink-Doselaar et al., 2009), no sex differences were assessed at P0. Next, brains were quickly removed from the skull and weighed. Dorsal views of whole brains were imaged using a Zeiss (Oberkochen/Germany) Axio high resolution (HRm) camera attached to a dissecting microscope. Cortical lengths were measured with a digital micrometer in ImageJ (NIH) using dorsal whole brain images. After post-fixation in 4% PFA, brains were hemisected and hemispheres were designated for either anatomy, gene expression assays, or dye tracing. Designated subsets of each litter were kept with their mothers until P20 where they were either used immediately in behavioral analysis, or were weaned until P30 where separate, alternate behavioral analyses took place. Table 1 summarizes the total animal usage and sex breakdown within the study.

Anatomical measurements.

For anatomical measurements of cortical areas (i.e. thickness), P0 hemispheres (PatEE n = 8 and P0 control n = 8) were cryoprotected in 30% sucrose solution for 1 to 3 days. Tissue was sectioned at 40 μm on the coronal plane via Leica cryostat, mounted, then stained for Nissl substance. Brain sections were imaged using a Zeiss Axio Upright Imager microscope equipped with a Zeiss Axio HRm camera. In order to make comparisons between groups, strict matching of sections took place using the Paxinos developing mouse brain atlas (Paxinos et al., 2007) as a guide as well as a number of anatomical landmarks including corpus callosum, hippocampus, and subcortical structures. Due to the stringent nature of such section matching, individual cases were only included in quantitative analysis for particular cortical areas if they met the exact-match criteria. Once matched, regions of interest (ROIs) were measured using an electronic micrometer in ImageJ (NIH) by a trained researcher blind to treatment, as previously reported (Abbott et al., 2016). Briefly, cortical thickness measurements were determined from electronic lines perpendicular to the cortical sheet, drawn from the most superficial region of layer I to the deepest region of layer VI. Regions measured included putative frontal cortex, prelimbic cortex, auditory cortex, putative somatosensory cortex (S1), and putative visual cortex (V1). All cortical thickness data were evaluated as a transformed percentage change from a baseline corrected control set at 100%.

Gene expression assays.

Analysis of gene expression within P0 brain hemispheres was carried out via *in situ* RNA hybridization (ISH). Standard protocols for free-floating non-radioactive ISH were used to visualize neocortical *Id2* and *RZRβ* gene expression of P0 control and PatEE brains, as previously described (Dye et al., 2011a; 2011b; El Shawa et al., 2013). Briefly, hemispheres were first embedded in gelatin-albumin, and sectioned at 100μm via vibratome. After hybridization to probes for *Id2* and *RZRβ* synthesized from cDNA (gifts from John Rubenstein, UCSF; see Abbott et al., 2018 for details), sections were mounted in a 50% glycerol solution onto glass slides, coverslipped, and imaged using a Zeiss Axio HRm camera attached to a dissecting microscope. Anatomically matched ISH sections from

PatEE and control P0 brains are presented to highlight the effects of altered gene expression of *Id2* and *RZRβ* associated with PatEE. Additionally, analysis of gene expression was also quantified at specific, highlighted ROIs, by calculating transcript densities using ImageJ (NIH). Briefly, images at identical anatomical levels were converted to binary and a standardized threshold was defined. ROIs were then defined by static electronic grid positioning over the specific cortical areas in both control and PatEE brains. Using landmarks such as hippocampus, anterior commissure, and corpus callosum, sections were matched carefully and multiple cases were used, as published previously, to ensure reliability (El Shawa et al., 2013). Individual transcript density signals (as pixel densities) were measured and reported as area fraction of total ROI.

Anatomical tracing.

To determine patterns of ipsilateral INC development in P0 mice 1,1-Dioctadecyl-3,3,3,3-tetramethylindocarbocyanine (DiI; Invitrogen, Carlsbad, CA/USA) and 4-(4-(dihexadecylamino)styryl)-N-methylpyridinium iodide (DiA; Invitrogen) dye crystals were placed in putative somatosensory (S1) or putative visual cortex (V1), as described previously (Dye et al., 2011a; 2011b; El Shawa et al., 2013). A coordinate grid was used for reliability of dye placement locations (DPLs) across cases. Following placement of crystals, hemispheres were placed in 4% PFA in the dark at 30°C for 4-6 weeks to allow for dye transport. Upon confirmation of retrograde thalamic nuclei labeling, brains were embedded in 5% low melting point agarose, and sectioned at 100μm via vibratome in 1X phosphate buffered saline. Sections were then counterstained with 4′, 6-diamidino-2-phenylindole dihydrochloride (DAPI; Roche, Basel/Switzerland), mounted onto glass slides, and coverslipped using FluoroMount (Sigma; St. Louis, MO/USA). A Zeiss Axio Upright Imager microscope equipped with a Zeiss Axio high resolution (HRm) camera and three filters was used to visualize and capture images of dye tracing sections via PC running Axiovision software (version 4.8). The three filters used are detailed in the following: red for DiI, green for DiA, and blue for DAPI counterstain labeling (Excitation wavelengths-red: Cyanine 3, 550 nm; green: green fluorescent protein (GFP), 470 nm; blue: DAPI, 359 nm. Emission

wavelengths-red: Cyanine 3, 570 nm; green: GFP, 509 nm; blue: DAPI, 461 nm). Images from all 3 filters per section were merged for subsequent analysis. Matched sections from PatEE and control brains using DAPI counter-stained landmarks were used to compare the development and trajectory of INCs between treatment groups.

Dye placement locations (DPLs) were quantified as a percentage of total cortical length to ensure that the relative size of the injection remained consistent. Dye projection zones (DPZs) in the visual and somatosensory cortices were quantified as a percentage of total cortical length by measuring the distance from the most rostral and caudal retrogradely labeled cells using a micrometer. Additionally, the lateral dispersion of cells stemming from V1 injections was quantified by electronically measuring the distance from the corpus callosum to the furthest laterally labeled cell in anatomically matched sections.

Behavioral assays. Behavioral assessment of PatEE and control offspring occurred via a battery of behavioral tests at pre- and peri-pubescence. All P20 control and PatEE mice were tested on the Suok assay and P30 mice were tested on the Accelerated Rotarod (AR), Forced Swim Test (FST) and Three-Chambered Sociability Test. For P30 behavior, all mice were randomly assigned to 2 of 3 assessments on the day of behavioral testing to reduce handling and stress. The Suok was used to assess anxiety and sensorimotor integration (Kalueff et al., 2008; see Supplemental Methods for details). AR (Ugo Basile; Gemonio/Italy) was used to test motor ability, learning, and coordination (Rustay et al., 2003; Buitrago et al., 2004; see Supplemental Methods). FST was used to screen for depressive-like behavior (Lucki et al., 2001; see Supplemental Methods). FST was always reserved as the final test due to the high-stress nature of the test. Lastly, the Three-Chambered Sociability test was used to examine social interaction behavior, or sociability (Yang et al., 2011; see Supplemental Methods). All behavioral analyses and scoring were accomplished by trained researchers blind to experimental condition.

Statistical analysis.

All statistical analyses were completed using GraphPad Prism 6 (La Jolla, CA/USA). For all sire measurements, pup measurements, and P0 pup brain analyses (ISH, dye-tracing, anatomy), unpaired two-tailed *t*-tests were used to compare results between control and experimental groups. For data displayed as percent change (i.e. cortical thickness measurements), mean baseline corrected control was set as 100%, with experimental (PatEE) measures expressed as percentage variation from that mean. In all behavioral measures except for P30 Accelerated Rotarod analysis, two-way analyses of variance (ANOVA) (factors: sex and treatment) followed by Tukey's post hoc test were used to assess group differences. For AR analysis, a two-way repeated measures ANOVA (factors: trial and treatment) followed by the Holm-Sidak post hoc test was used to evaluate group differences. Additionally, for AR analysis, a three-way repeated measures ANOVA (factors: sex, trial, treatment) was used to directly examine potential sex differences and three-way interactions. For all statistical measures, a p value of < 0.05 was set for significance. All data are expressed as mean ± S.E.M. and these values are presented in Table 2.

RESULTS

Paternal measurements.

In order to assess potential differences in liquid intake among EtOH-exposed and control fathers, we measured liquid intake daily for the length of exposure (Fig. 2). We found no significant differences in daily liquid intake between control and EtOH-exposed sires (Fig. 2A, $p = 0.560$). We also found no significant differences in total weight gain during the exposure period between control and EtOH-exposed sires or in daily average food intake (Table 2; $p = 0.7748$, $p = 0.1191$, respectively). To confirm EtOH exposure, as well as measure the level of EtOH intoxication, we measured blood EtOH concentration (BECs) in 7 males exposed to 25% EtOH for 20 days, as well as 7 control males (Fig. 2). The 20-day exposure time point was chosen to measure BECs due to it being near average position in the 15-23 day exposure paradigm used. As expected, sires exposed to 20 days of 25% EtOH showed elevated BEC levels and control (water exposed) sires did not display any detectable BEC levels (Fig. 2B, $^{**}p < .01$). Overall, these results suggest that no disparity in

liquid intake, food intake, or weight gain occurs due to EtOH exposure in sire mice, and that sufficient levels of EtOH intoxication occur in male mice following a 20-day exposure period.

P0 pup and dam measurements.

To examine the ability of PatEE to produce gross alterations in pup CNS development, we evaluated brain weights and total cortical lengths in control and PatEE offspring at P0. No significant differences were present in newborn brain weights (Fig. 3A, $p = 0.811$) or cortical lengths (Fig. 3B, $p = 0.31$) between PatEE and control mice.

Additionally, due to EtOH's ability to reduce overall litter sizes in CD-1 mice following maternal EtOH exposure (El Shawa et al., 2013), we measured control and PatEE litter sizes and found no differences in litter size due to PatEE (Fig. 3C, $p = 0.932$). Overall, these results suggest that a moderate paternal exposure does not produce gross alterations in CNS development in pups at P0, as well as differences in litter size/viability in non-directly EtOH exposed dams.

Cortical anatomical measurements.

PatEE in rats has been shown to generate altered cortical thickness in P28 offspring (Jamerson et al., 2004). In order to assess the effects of a 15-23 day PatEE on cortical thickness development at P0, we measured from 5 distinct regions in Nissl-stained coronal sections in both control and PatEE mice (Fig. 4). These regions included putative frontal, prelimbic, somatosensory, auditory, and visual cortices. No significant differences in cortical thickness were observed in PatEE mice compared to controls in frontal cortex (Fig. 4A, $p = 0.9008$), prelimbic cortex (Fig. 4B, $p = 0.6644$), somatosensory cortex (Fig. 4C, $p = 0.1670$), auditory cortex (Fig. 4D, $p = 0.1647$), or visual cortex (Fig. 4E, $p = 0.8813$). Together, these results suggest that a moderate 15-23 day paternal ethanol exposure does not impact cortical thickness development in mice at P0.

Cortical gene expression analyses.

Id2 and *RZRβ* are two genes important for neocortical patterning and arealization (Rubenstein et al., 1999). Previously, we demonstrated that cortical expression of these two genes is altered by maternal prenatal EtOH exposure at P0 (El Shawa et al., 2013; Abbott et al., 2018). Accordingly, we investigated expressions of *Id2* and *RZRβ* in neocortex to determine whether this patterning is affected by PatEE in mice at P0. Using *in situ* RNA hybridization, we examined patterns of gene expression in P0 coronal hemisections via side-by-side analyses of anatomically matched sections from both control and PatEE brains (Fig. 5). In control mice, *Id2* expression is highly complex, spanning multiple cortical layers including II/III, V, and VI (Fig. 5A1-5). Additionally, a distinct boundary of the most superficial *Id2* expression occurs in control mice at P0 (arrows, Fig. 5A2-3), which marks the border of absent lateral *Id2* expression. In anatomically matched sections of PatEE mice, however, this border appears to be visually shifted to further lateral cortical regions (arrows, Fig. 5B2-3), and, thus, *Id2* expression also extends further laterally compared to controls. *RZRβ* expression in control animals is largely limited to cortical layer IV (Fig. 5C1-5). However, a typical border occurs that delineates an absence of expression in the medial cortical wall (arrow, Fig. 5C3). In contrast, PatEE brains exhibit a medial shift in this boundary (arrow, Fig. 5C4), and *RZRβ* expression extends medially as a result.

In order to quantify and confirm these visually identified cortical gene expression shifts, we used binary-converted images of raw data to measure density of transcript within static ROIs in both control and PatEE anatomically matched sections (Fig. 6). *RZRβ* expression was quantified in the medially positioned ROI (black box) designated within the line drawing (Fig. 6C1). As seen in the representative ISH images (Fig. 6A1; B1), medial expression of *RZRβ* was increased significantly in the ROI in the rostral region of parietal cortex in PatEE mice compared to controls at P0 (Fig. 6D1, $p < .01$). *Id2* expression was similarly quantified within a static ROI, however this ROI was positioned further laterally (black box, Fig. 6C2). *Id2* expression was increased significantly within the ROI in PatEE brains compared to controls (Fig. 6D2, $p < .0001$).

Importantly, these concurrent shifts in both *Id2* and *RZRβ* cortical boundaries of expression occur at the same anatomical levels i.e. both shifts were quantified in

anatomically matched sections among both groups (compare representative images and line drawings in Fig. 6A1, B1, C1 to Fig. 6A2, B2, C2). As seen in control mice, *RZRβ* and *Id2* expression boundaries approximately abut each other near the visual-sensory cortex border at P0 (compare arrow in Fig. 6A1 to arrow in Fig. 6A2). However, in PatEE mice, both of these two boundaries of expression extend in opposite directions i.e. *RZRβ* extends medially and *Id2* expression extends laterally (compare arrow in Fig. 6B1 to arrow in Fig. 6B2), producing an atypical overlapping region of expression.

Dye tracing experiments.

Ipsilateral intraneocortical connections (INCs) constitute a distinct feature of mature cortical areas (Kaas, 1982) and prenatal EtOH results in disorganized INC patterns within the cortex of exposed P0 mice (El Shawa et al., 2013; Abbott et al., 2018). Here, we characterized development of ipsilateral INCs in control and PatEE brains at P0 using lipophilic dyes (Fig. 7). and present the patterns of INCs stemming from putative S1 (asterisks, Fig. 7A2, B2) and putative V1 dye placements (asterisks, Fig. 7A5, B5). No significant differences in dye placement locations (DPLs) in the putative S1 (Fig. 8A, $p = 0.78$) and putative V1 (Fig. 8C, $p = 0.15$) were observed, ensuring that the relative injection size was consistent across cases.

No significant differences in dye projection zones (DPZs) of the somatosensory cortex were observed (Fig. 8B, $p = 0.289$), as well as in visual cortex DPZs, although a trend towards significance was noted (Fig. 8D, $p = 0.09$). However, PatEE brains contained aberrant labeled cells in rostral regions not present in controls (Fig. 7B3), which were present in variable amounts in PatEE mice. Additionally, in control mice, labeled S1-derived cells extend caudally, and are located laterally to the visual cortex forming the somatosensory-visual boundary in controls (Fig. 7A4). However, a clear boundary between these regions was not consistently observed in PatEE mice, as some mixing between S1-derived and V1-derived cells was present (Fig. 7B3, B4). In order to quantify this phenomenon, we used a novel technique to measure the lateral cortical cell dispersion at this region and found that labeled cells stemming from V1 injections are present in further lateral cortical positions in PatEE mice compared to controls (Fig. 9, $p = 0.0410$), suggesting

abnormal patterning of INCs at P0 due to PatEE. Interestingly, this areal cell mixing was also seen at the same anatomical level of the abnormal *RZRβ* and *Id2* overlapping region observed at P0 in PatEE mice (compare levels: Fig. 6A1-2, B1-2 to Fig. 7A4, B4). These data suggest that PatEE results in subtle alterations in INC patterns in newborn mice, which may be related to altered cortical patterning gene expression.

P20 behavioral analysis.

To assess PatEE's impact on behavioral development, we used a battery of behavioral tests at two ages in PatEE and control mice. At P20, we assessed behavior using the Suok test, a succinct behavioral test which can assess both sensorimotor integration/function and anxiety-like behavior (Kalueff et al., 2008). Two measures of sensory motor integration, missteps and falls, were evaluated during the singular 5-minute trial of the Suok. A two-way ANOVA revealed a significant main effect of treatment for missteps [$F_{(1,53)} = 18.57$, $p < 0.0001$] but no main effect of sex. Post-hoc analyses revealed an increase in missteps in female PatEE mice compared to female controls (Fig. 10B, $p < .005$), as well as a statistical trend in increased missteps for PatEE vs. control males (Fig. 10B, $p = 0.057$). Additionally, there was no sex × treatment interaction for missteps. There were no main effects of sex or treatment for falls and no sex × treatment interaction (Fig. 10A). Additionally, there was a significant main effect of treatment on segments crossed [$F_{(1,53)} = 13.74$, $p = 0.0005$], and post hoc analyses revealed an increase in the number of segments crossed in PatEE vs. control males (Fig. 10C, $p < .01$) but not for PatEE vs. control females. There was no main effect of sex for segments crossed and no sex × treatment interaction.

Anxiety-like behaviors including rearing/grooming events, directed exploration, and latency to leave the center of the bar were also evaluated using the Suok test. Two-way ANOVA analyses revealed no significant main effects of sex or treatment or sex × treatment interactions for rearing/grooming events (Fig. 10D), latency to leave center (Fig. 10F) or directed exploration events (Fig. 10E). Overall, results suggest that 15-23 days of PatEE can produce altered behavior at P20 in a sex-specific manner, including increased activity in males and perturbed sensorimotor integration in both males and females.

P30 behavioral analysis.

We examined behavior at P30 in control and PatEE mice using several different tasks including the Accelerated Rotarod (AR) for motor learning (Rustay et al., 2003), Forced Swim Test (FST) for depressive-like behavior (Lucki et al., 2001), and Three-Chambered Sociability Test for social behavior and interaction (Yang, et al., 2011; Fig. 11).

For males, a two-way repeated measures ANOVA showed significant main effects of both trial [$F_{(3,69)} = 20.16$, $p < 0.0001$] and treatment [$F_{(1,23)} = 8.2889$, $p = 0.0085$] on time on the accelerating rod in the AR test. Holm-Sidak post hoc analysis revealed a significant decreased time for PatEE males compared to control males within trials 2 ($p < .01$) and 3 ($p < .05$). Additionally, although both male groups show a significant increase in performance across all 4 trials (trial 1 vs. trial 4; control males: $p < 0.0001$, PatEE males: $p < 0.0001$), only control mice display a significant increase in performance between trials 1 and 2 (control males: $p = 0.0002$, PatEE males: $p = 0.0950$), indicating a potential impairment in short-term motor learning in males due to PatEE. There was no trial × treatment interaction effect observed in the 2-way ANOVA for males. In contrast, in females, two-way repeated measures ANOVA revealed a significant main effect of trial [$F_{(3,75)} = 9.373$, $p < 0.0001$], but not in treatment [$F_{(1,25)} = 0.1744$, $p = 0.6798$], as both female control and PatEE mice increased performance across all trials (trial 1 vs. trial 4; control females: $p = 0.0035$, PatEE females: $p = 0.0072$). As with the males, there was no trial × treatment interaction effect observed in the two-way ANOVA for females. Additionally, a three-way repeated measures ANOVA was performed to examine potential sex differences directly. This test indeed revealed a significant main effect of sex [$F_{(1,48)} = 5.722$, $p = 0.021$], as well as trial [$F_{(3,124)} = 29.46$, $p < 0.0001$], and treatment [$F_{(1,48)} = 5.916$, $p = 0.019$], for time on the accelerating rod in the AR test. This indicates that collapsing across treatment and trial, males performed worse when compared to females and, collapsing across sex and trial, PatEE mice performed worse compared to controls. No trial × treatment × sex interactions were observed.

In the FST, time spent immobile was used as a measure for depressive-like behaviors (Fig. 11C) and a two-way ANOVA revealed no significant main effects of treatment or sex and no sex × treatment interaction. Lastly, a two-way ANOVA for the sociability test revealed no significant main effects of treatment or sex and no sex × treatment interaction between control and PatEE mice in the amount of time spent with the novel mouse (Fig. 11D), indicating social interaction abnormalities do not result from 15-23 days of PatEE in our model. Together, these data suggest that PatEE also generates behavioral abnormalities at P30, including sensorimotor and short-term motor learning impairments.

DISCUSSION

In this study, we demonstrate that paternal ethanol exposure can induce dramatic alterations in offspring neocortical gene expression and subtle changes in neocortical connectivity. Additionally, behavioral testing indicated that PatEE male mice display increased activity, as well as impaired coordination and short-term motor-learning abilities. Furthermore, female PatEE mice displayed deficits in sensorimotor integration. Overall, these results suggest that 15-23 days of PatEE can alter brain and behavioral developmental trajectories in rodent offspring.

PatEE and general offspring development: human and rodent models

The deleterious effects of PatEE, while markedly understudied in comparison to PrEE via maternal EtOH consumption during pregnancy, have been examined for over 100 years (Stockard and Papanicolaou, 1918). In humans, children of alcoholic fathers have been shown to display cognitive impairments (Tarter et al., 1989). Additionally, PatEE in humans has been associated with lower birth weights (Little and Sing, 1987), increased risk of congenital defects (Zuccolo et al., 2017), and altered reproductive development (Xia et al., 2018), suggesting PatEE may be more impactful on offspring development than previously thought.

Rodent studies, using a variety of species, strains and exposure paradigms, have generally reinforced this idea. Researchers have described various behavioral abnormalities

(Abel and Lee, 1988; Abel, 1991; Jamerson et al., 2004; Meek et al., 2007; Kim et al., 2014; Hollander et al., 2019), as well as lower weights at birth (Bielawski et al., 2002), increased incidence of runts in litters (Bielawski and Abel, 1997), smaller litter sizes (Meek et al., 2007; Liang et al., 2014), and congenital CNS anomalies (Lee et al., 2013).

In the current study, we do not report any litter size or gross brain/body weight changes at birth due to PatEE. These apparent differences may be related to the length or dosage of exposure, as some previous studies were designed to encapsulate at least one cycle of spermatogenesis within sires (~35 days; Adler, 1996). However, duration of PatEE has not always predicted litter size alterations, as a 6-month exposure did not result in any significant differences in PatEE offspring litter size (Ceccanti et al., 2016). An alternative explanation is that differences could be species and strain-specific, as Ceccanti and colleagues also utilized the same strain used within our study (CD-1 mice).

Neocortical development- thickness by region

Here, we found that 15-23 days of PatEE produced no significant effect on cortical thickness in any putative area measured, including frontal, prelimbic, somatosensory, visual, and auditory cortices. Very few rodent models have examined the impact of PatEE on neocortex; however, a study by Jamerson and colleagues (2004) examined cortical thickness in adolescent PatEE rats whose sires received a long-term EtOH exposure. These PatEE rats displayed significant increases in frontal cortical thickness. While our P0 mouse PatEE offspring do not display such frontal cortical enlargement, this discrepancy could be explained by the age of measurement. An alternate, distinct possibility could be that altered cortical thickness described previously would be manifested in our model at later ages; this will be addressed in future studies.

Impact of PatEE on cortical gene expression and INC development

In previous rodent models, PatEE has been shown to disturb gene expression in the brain (Liang et al., 2014; Finegersh and Homanics, 2014; Przybycien-Szymanska et al., 2014; Kim et al., 2014; Rompala et al., 2017) and liver (Chang et al., 2017; 2019) of offspring. In this

study, we examined two specific genes involved in governing arealization, and found that both *RZRβ* and *Id2* expression were altered in the cortex of P0 offspring sired by male mice exposed to EtOH. Functionally, *Id2* is a helix-loop-helix transcription factor important for neural stem cell renewal and normal CNS development (Park et al., 2013), while *RZRβ,* a nuclear receptor*,* influences proper cortical structural patterning, including development of the barrel cortex in S1 (Jabaudon et al., 2012). Importantly, both genes are present within murine cortex at embryonic and early postnatal ages and are expressed in distinct layer and area-specific patterns, suggesting their role in arealization (Rubenstein et al., 1999; Dye et al., 2011a). In particular, *Id2* and *RZRβ* expression boundaries have been implicated in guidance of regional development of early INCs (Huffman et al., 2004). Within our model, transcript densities of cortical *Id2* and *RZRβ* were increased in specific ROIs in PatEE mice. Particularly, we observed a lateral shift in Id2 expression and a medial shift in *RZRβ* expression that co-registered at the same anatomical level. This anatomical co-registration results in *Id2* and *RZRβ* expression in PatEE neocortices that overlap each other in a way that is not typically seen in control mice.

We examined the functional significance of this overlapping region using tracing of INCs via lipophilic dyes. We found that PatEE produces subtle changes in INC development at P0, including a distinct mixing of putative V1 and S1 projection zones that is not present in normal, developing mice. At the somatosensory-visual border, control mice display a clear border at this region but, in PatEE mice, the boundaries of this border show overlapping connections. As this region also corresponds to the level of overlapping *Id2* and *RZRβ* expression, we propose that the shift in expression may underlie the altered INC patterns seen in newborn PatEE mice. To our knowledge, this is the first study reporting concurrent altered cortical genetic and neuronal patterning in the context of PatEE.

Results from the current study are also interesting in comparison to PrEE results. In newborn PrEE mice, whose mothers consumed 25% EtOH throughout pregnancy, we observe consistent shifts in *Id2* and *RZRβ* expression, severely disrupted INC patterns, and altered behavior at later ages (El Shawa et al., 2013; Abbott et al., 2018). Although PatEE may not result in the level of disruption in INC development seen in our PrEE model, similar

mechanisms may be affected. Overall, we suggest that a 15-23 day paternal exposure directly before conception results in subtle changes in INC connectivity that may be due to shifted cortical gene expression patterns. As patterns of INCs remain a characteristic component of cortical area form and function (Kaas, 1982), subtle changes in INC development due to PatEE may underlie (or contribute to) behavioral changes seen in rodents (reviewed in Finegersh et al., 2015), as well as in human children of alcoholic fathers (Tarter et al., 1989; Knopik et al., 2005).

PatEE and sex-specific behavioral development

Here, we found that PatEE male mice display increased activity, which may be reflective of a hyperactive phenotype, compared to male control mice as shown by increased segments crossed in the Suok test. These results support findings in previous reports that indicate that PatEE can cause expression of attention deficit hyperactivity disorder (ADHD)-like behavioral phenotypes, as assessed via increased activity and impulsivity measures in rodents (Ledig, et al., 1998; Kim et al., 2014). Specifically, Kim and colleagues (2014) found that male PatEE mouse offspring display increased open field activity, suggesting that male offspring may be particularly prone to increased activity or hyperactive behaviors imparted by paternal drinking. Additionally, our results potentially corroborate the clinical finding that ADHD incidence is increased in the children of alcoholic fathers (Knopik et al., 2005). Interestingly, ADHD prevalence in children prenatally exposed to EtOH via maternal consumption ranges between 49.4% and 94%, exhibiting the highest comorbidity in FASD patients (Bhatara et al., 2006; Fryer et al., 2007). This suggests that PatEE and PrEE may disrupt behavioral phenotypes in comparable manners. However, rodent models have also reported hypoactivity in PatEE offspring (Abel, 1989), obscuring the push towards a unified PatEE behavioral phenotype. Further work must be done in order to clarify this challenging prospect, especially from a sex-specific standpoint.

Additionally, we report sex-specific decreased sensorimotor integration and motor coordination at both P20 and P30 due to PatEE. Specifically, we found that PatEE female offspring show increased missteps in the Suok at P20 and PatEE male mice display

decreased total time on the AR in trials 2 and 3 at P30. Although motor coordination and sensorimotor integration are consistently altered by maternal EtOH exposure in humans (Doney et al., 2014), much less is known of the impact of PatEE. Our results support findings of decreased balance in early postnatal pups due to PatEE (Jamerson et al., 2004), and expand on these by providing evidence of later-age behavioral impairment, and potentially of the impact on short-term motor learning. Using a single-day, multi-session AR paradigm, motor coordination and short-term learning can be assessed simultaneously (Buitrago et al., 2004). Despite significantly lower scores in trials 2 and 3, male PatEE mice are not significantly different from male control counterparts in trial 4, suggesting that motor learning may be acutely hindered due to PatEE. These results support the ability of PatEE to negatively impact various aspects of learning (Wozniak et al., 1991; Liang et al., 2014). Together, our data confirm the ability of PatEE to impact both learning in offspring, as well as in general motor coordination and sensorimotor integration, further solidifying the negative impact of PatEE on offspring behavior. However, the sex- and age-specific findings of the current study highlight the complexity of the outcomes that can result due to PatEE.

Impaired social behaviors have been widely described in both rodent (Hamilton et al., 2010) and human studies (Thomas et al., 1998) of PrEE offspring. We assessed social behavior in our PatEE model to determine if preconception EtOH exposure in the sire results in similar consequences using the social interaction test. However, we found no significant differences in time spent in the chamber with a novel mouse, regardless of sex, indicating PatEE mice do not display altered social interaction behaviors compared to control mice at P30 in our model. Although, to our knowledge, no previous reports have examined social interaction behaviors in PatEE offspring, others have found increased aggression in PatEE male offspring (Meek et al., 2007). Together, these results suggest that PatEE may alter specific facets of social behavior. Due to the complexity and wide range of social behaviors in rodents, future studies must attempt to fully describe the impact of PatEE on offspring social behaviors to provide a more complete assessment.

Lastly, anxiety-like and depressive-like behaviors were also assessed via the Suok and FST, respectively. However, no differences were found in PatEE mice compared with

controls in all three Suok measures of anxiety-like behavior or in depressive-like behavior, regardless of sex. This contrasts to a previous report indicating increased anxiety-like and depressive-like behaviors in mice offspring whose fathers were exposed to 4 weeks of EtOH exposure (Liang et al., 2014). However, alternate studies reported no differences in offspring basal anxiety levels due to PatEE (Finegersh and Homanics, 2014; Rompala et al., 2017; Beeler et al., 2019). Collectively, these results suggest that impact of PatEE on rodent offspring anxiety-like and depressive-like behaviors are complex, and their manifestation may rely on multiple factors including sex, strain, treatment type, length, and dosage.

Possible mechanisms underlying PatEE's effects on offspring

Although the current study characterized the alterations in offspring brain and behavior due to PatEE, several previous studies have examined potential mechanisms for transmission of PatEE's harmful effects from sperm to offspring (for more details, please see review by Rompala and Homanics, 2019). Because EtOH is a known disruptor of epigenetic regulation in both adult (Cervera-Juanes et al., 2017) and prenatal exposure (Garro et al., 1991) contexts, most research has focused on the potential mechanism of PatEE germ cell alteration as one that is epigenetically mediated. This hypothesis has also been supported by studies that have shown EtOH exposure alters DNA methylation (Bielawski et al., 2002), histone acetylation (Kim and Shukla, 2006), and small noncoding RNA profiles (Rompala et al., 2018) of rodent male sperm cells and/or testis. This hypothesis is especially compelling considering human sperm cell DNA hypomethylation of typically hypermethylated imprinted genes is associated with EtOH consumption (Ouko et al., 2009).

PatEE rodent model studies have examined this question of mechanism and have found various results revealing EtOH's effect on spermatogenesis. For example, Liang and colleagues (2014) reported DNA methylation decreases at paternally imprinted genes in EtOH-exposed sire sperm. However, other studies have found no evidence for PatEE's effects being mediated through epigenetic regulation of imprinted genes (Chang et al., 2017; 2019), suggesting other epigenetic mechanisms may underlie observed effects on offspring brain and behavior. Because small noncoding RNAs (sncRNAs), such as microRNAs,

transfer RNA-derived RNAs, and mitochondrial small RNAs, are present in male gametes (Krawetz et al., 2011), these have also been hypothesized to play a key role in PatEE. In fact, a recent study has confirmed that paternal exposure alters expression of several of these sncRNAs in male sperm (Rompala, et al., 2018).

While the exact mechanisms and molecular players are still unclear, evidence points towards an epigenetically mediated alteration of EtOH-exposed sperm. Extrapolating data from the current study, we hypothesize that PatEE may cause sperm cell epigenetic dysregulation, which in turn may result in gene expression alterations within offspring brain (such as in *Id2* and *RZRβ* expression), resulting in altered cortical patterning and ectopic development of neocortical circuits (such as the mixing of S1 and V1 intraneocortical connections). We suggest that the altered neuronal patterning may underlie the abnormal behavior seen within the current study and others. A graphical abstract of the proposed model is seen in Fig. 12.

Conclusions

We report altered gene expression and intraneocortical connectivity in newborn mice (PatEE) sired by males that had 15-23 days of preconception exposure to EtOH with correlative behavioral abnormalities in juveniles. Additionally, PatEE mice exhibited behavioral alterations consistent with some documented human patterns of behavior of children born to fathers who were alcoholics. Finally, there appear to be differential effects of PatEE on male versus female offspring. In general, male offspring seem to be more adversely affected by the paternal ethanol exposure when compared to females.

Future directions include examining epigenetic regulation of *Id2* and *RZRβ* within the cortex of PatEE mice to further discern potential mechanisms, as well as extending the current study to later ages to determine if the reported differences in offspring brain and behavior are transient or long-lasting. Also, since many prenatal ethanol exposure phenotypes have been shown to pass transgenerationally (Abbott et al., 2018; see review by Chastain and Sarkar, 2017), an investigation of whether the observed phenotypes and sex differences from preconception PatEE also persist into future generations beyond the F1

generation should occur. In conclusion, our data support the notion that the preconception paternal environment is more impactful on offspring development than previously thought, and that paternal EtOH exposure may cause harmful consequences in offspring.

ACKNOWLEDGEMENTS

The authors thank Mirembe Nabatanzi for help with behavioral experiments and histology, Roberto F. Perez Jr. for assistance in behavioral data collection and David J. Rohac for assistance in anatomy measurements. We also thank Joe Valdez, Jim McBurney-Lin, and Sarah Maples for help in data collection. All authors are free of any conflict of interests.

REFERENCES

Abbott CW, Kozanian, OO, Kanaan, J, Wendel, KM, Huffman, KJ (2016) The impact of prenatal ethanol exposure on neuroanatomical and behavioral development in mice. Alcohol Clin Exp Res 40:122–133.

Abbott CW, Rohac DJ, Bottom RT, Patadia S, Huffman KJ (2018) Prenatal ethanol exposure and neocortical development: a transgenerational model of FASD. Cereb Cortex 28:2908–2921.

Abel EL, Lee JA (1988) Paternal alcohol exposure affects offspring behavior but not body or organ weights in mice. Alcohol Clin Exp Res 12:349–55.

Abel EL (1989) Paternal alcohol consumption: Effects of age of testing and duration of paternal drinking in mice. Teratology 40:467–474.

Abel EL (1991) Alcohol consumption does not affect fathers but does affect their offspring in the forced swimming test. Pharmacol Toxicol 68:68–69.

Adler ID (1996) Comparison of the duration of spermatogenesis between male rodents and humans. Mutat Res Mol Mech Mutagen 352:169–172.

Bielawski DM, Abel EL (1997) Acute treatment of paternal alcohol exposure produces malformations in offspring. Alcohol 14:397–401.

Bielawski DM, Zaher FM, Svinarich DM, Abel EL (2002) Paternal alcohol exposure affects sperm cytosine methyltransferase messenger RNA levels. Alcohol Clin Exp Res 26:347–351.

Beeler E, Nobile L, Homanics, GE (2019) Paternal preconception every-other-day ethanol drinking alters behavior and ethanol consumption in offspring. Brain Sci 9:56.

665 Bhatara V, Loudenberg R, Ellis R (2006) Association of attention deficit hyperactivity
666 disorder and gestational alcohol exposure. J Atten Disord 9:515–522.

667 Buitrago MM, Schulz JB, Dichgans J, Luft AR (2004) Short and long-term motor skill learning
668 in an accelerated rotarod training paradigm. Neurobiol Learn Mem 81:211-216.

669 Ceccanti M, Coccurello R, Carito V, Ciafrè S, Ferraguti G, Giacovazzo G, Mancinelli R,
670 Tirassa P, Chaldakov G N, Pascale E, Ceccanti M, Codazzo C, Fiore M (2016) Paternal
671 alcohol exposure in mice alters brain NGF and BDNF and increases ethanol-elicited
672 preference in male offspring. Addict Biol 21:776–787.

673 Cervera-Juanes R, Wilhelm LJ, Park B, Grant KA, Ferguson B (2017) Genome-wide
674 analysis of the nucleus accumbens identifies DNA methylation signals differentiating
675 low/binge from heavy alcohol drinking. Alcohol 60:103–113.

676 Chang RC, Skiles WM, Chronister SS, Wang H, Sutton GI, Bedi YS, Snyder M, Long CR,
677 Golding MC (2017). DNA methylation-independent growth restriction and altered
678 developmental programming in a mouse model of preconception male alcohol
679 exposure. Epigenetics 12:841–853.

680 Chang RC, Wang H, Bedi Y, Golding MC (2019) Preconception paternal alcohol exposure
681 exerts sex-specific effects on offspring growth and long-term metabolic programming.
682 Epigenetics Chromatin 12:9.

683 Chastain LG, Sarkar DK (2017) Alcohol effects on the epigenome in the germline: Role of
684 inheritance of alcohol-related pathology. Alcohol 60:53-66.

685 Dye CA, El Shawa H, Huffman KJ (2011a) A lifespan analysis of intraneocortical
686 connections and gene expression in the mouse I. Cereb Cortex 21:1311–1330.

687 Dye CA, El Shawa H, Huffman KJ (2011b) A lifespan analysis of intraneocortical
688 connections and gene expression in the mouse II. Cereb Cortex 21:1331–1350.

689 Doney R, Lucas BR, Jones T, Howat P, Sauer K, Elliott EJ (2014) Fine motor skills in
690 children with prenatal alcohol exposure or fetal alcohol spectrum disorder. J Dev Behav
691 Pediatr 35:598-609.

692 El Shawa H, Abbott CW, Huffman KJ (2013) Prenatal ethanol exposure disrupts
693 intraneocortical circuitry, cortical gene Expression, and behavior in a mouse model of
694 FASD. J Neurosci 33:18893–18905.

695 Finegersh A, Homanics GE (2014) Paternal alcohol exposure reduces alcohol drinking and
696 increases behavioral sensitivity to alcohol selectively in male offspring. PLoS One
697 9:e99078.

698 Finegersh A, Rompala GR, Martin DIK, Homanics GE (2015) Drinking beyond a lifetime:
699 New and emerging insights into paternal alcohol exposure on subsequent generations.
700 Alcohol 49:461–470.

701 Fryer SL, McGee CL, Matt GE, Riley EP, Mattson SN (2007) Evaluation of
702 psychopathological conditions in children with heavy prenatal alcohol exposure.
703 Pediatrics 119:e733–e741.

704 Garro AJ, McBeth DL, Lima V, Lieber CS (1991) Ethanol consumption inhibits fetal DNA
705 methylation in mice: implications for the fetal alcohol syndrome. Alcohol Clin Exp Res
706 15:395–398.

707 Granato A, Di Rocco F, Zumbo A, Toesca A, Giannetti S (2003) Organization of cortico-
708 cortical associative projections in rats exposed to ethanol during early postnatal life.
709 Brain Res Bull 60:339–44.

710 Greenham LW, Greenham V (1977) Sexing mouse pups. Lab Anim. 11: 181-184.

711 Hamilton DA, Akers KG, Rice JP, Johnson TE, Candelaria-Cook FT, Maes LI, Rosenberg M,
712 Valenzuela CF, Savage DD (2010) Prenatal exposure to moderate levels of ethanol

alters social behavior in adult rats: Relationship to structural plasticity and immediate early gene expression in frontal cortex. Behav Brain Res 207:290–304.

Hollander J, McNivens M, Pautassi RM, Nizhnikov ME (2019) Offspring of male rats exposed to binge alcohol exhibit heightened ethanol intake at infancy and alterations in T-maze performance. Alcohol 76:65–71.

Hoyme HE, Kalberg WO, Elliott AJ, Blankenship J, Buckley D, Marais A-S, Manning MA, Robinson LK, Adam MP, Abdul-Rahman O, Jewett T, Coles CD, Chambers C, Jones KL, Adnams CM, Shah PE, Riley EP, Charness ME, Warren KR, May PA (2016) Updated clinical guidelines for diagnosing Fetal Alcohol Spectrum Disorders. Pediatrics 138:e20154256–e20154256.

Huffman KJ, Garel S, Rubenstein JLR (2004) Fgf8 regulates the development of intra-neocortical projections. J Neurosci 24:8917–8923.

Ikonomidou C, Bittigau P, Ishimaru MJ, Wozniak F, Koch C, Genz K, Price MT, Stefovska V, Tenkova T, Dikranian K, Olney JW (2000) Ethanol-induced apoptotic neurodegeneration and Fetal Alcohol Syndrome. Science 287:1056–1060.

Jabaudon DJ, Shnider SJ, Tischfield DJ, Galazo M, Macklis JD (2012) RORβ induces barrel-like neuronal clusters in the developing neocortex. Cereb Cortex 22:996–1006.

Jamerson PA, Wulser MJ, Kimler BF (2004) Neurobehavioral effects in rat pups whose sires were exposed to alcohol. Dev Brain Res 149:103–111.

Kaas JH 1982. The segregation of function in the nervous system: why do sensory systems have so many subdivisions? Contrib Sens Physiol 7:201-240.

Kalueff AV, Keisala T, Minasyan A, Kumar SR, LaPorte JL, Murphy DL, Tuohimaa P (2008) The regular and light–dark Suok tests of anxiety and sensorimotor integration: utility for behavioral characterization in laboratory rodents. Nat Protoc 3:129–136.

737 Kim J-S, Shukla SD (2006) Acute in vivo effect of ethanol (binge drinking) on histone H3
738 modifications in rat tissues. Alcohol Alcohol 41:126–132.

739 Kim P, Choi CS, Park JH, Joo SH, Kim SY, Ko HM, Kim KC, Jeon SJ, Park SH, Han S-H,
740 Ryu JH, Cheong JH, Han JY, Ko KN, Shin CY (2014) Chronic exposure to ethanol of
741 male mice before mating produces attention deficit hyperactivity disorder-like phenotype
742 along with epigenetic dysregulation of dopamine transporter expression in mouse
743 offspring. J Neurosci Res 92:658–670.

744 Knopik VS, Sparrow EP, Madden PAF, Bucholz KK, Hudziak JJ, Reich W, Slutske WS,
745 Grant JD, McLaughlin TL, Todorov A, Todd RD, Heath AC (2005) Contributions of
746 parental alcoholism, prenatal substance exposure, and genetic transmission to child
747 ADHD risk: a female twin study. Psychol Med 35:625–635.

748 Krawetz SA, Kruger A, Lalancette C, Tagett R., Anton E, Draghici S, Diamond MP (2011) A
749 survey of small RNAs in human sperm. Hum Reprod 26:3401–3412.

750 Krubitzer L, Huffman KJ (2000) Arealization of the neocortex in mammals: Genetic and
751 epigenetic contributions to the phenotype. Brain Behav Evol 55:322–335.

752 Ledig M, Misslin R, Vogel E, Holownia A, Copin J, Tholey G (1998) Paternal alcohol
753 exposure: developmental and behavioral effects on the offspring of rats.
754 Neuropharmacology 37:57–66.

755 Lee HJ, Ryu J-S, Choi NY, Park YS, Kim YI, Han DW, Ko K, Shin CY, Hwang HS, Kang K-
756 S, Ko K (2013) Transgenerational effects of paternal alcohol exposure in mouse
757 offspring. Animal Cells Syst 17:429–434.

758 Liang F, Diao L, Liu J, Jiang N, Zhang J, Wang H, Zhou W, Huang G, Ma D (2014) Paternal
759 ethanol exposure and behavioral abnormities in offspring: Associated alterations in
760 imprinted gene methylation. Neuropharmacology 81:126–133.

761 Little RE, Sing CF (1987) Father's drinking and infant birth weight: report of an association.
762 Teratology 36:59–65.

763 Lucki I, Dalvi A, Mayorga AJ (2001) Sensitivity to the effects of pharmacologically selective
764 antidepressants in different strains of mice. Psychopharmacology 155:315–22.

765 May PA, Chambers CD, Kalberg WO, Zellner J, Feldman H, Buckley D, Kopald D, Hasken,
766 JM, Xu R, Honerkamp-Smith G, Taras H, Manning MA, Robinson LK, Adam MP, Abdul-
767 Rahman O, Vaux K, Jewett T, Elliott AJ, Kable JA, Akshoomoff N, Daniel F, Arroyo JA,
768 Hereld D, Riley EP, Charness ME, Coles CD, Warren KR, Jones KL, Hoyme HE (2018)
769 Prevalence of fetal alcohol spectrum disorders in 4 US communities. J Am Med Assoc
770 319:474–482.

771 Meek LR, Myren K, Sturm J, Burau D (2007) Acute paternal alcohol use affects offspring
772 development and adult behavior. Physiol Behav 91:154–160.

773 Ouko LA, Shantikumar K, Knezovich J, Haycock P, Schnugh DJ, Ramsay M (2009) Effect of
774 alcohol consumption on CpG methylation in the differentially methylated regions of H19
775 and IG-DMR in male gametes: implications for fetal alcohol spectrum disorders. Alcohol
776 Clin Exp Res 33:1615–27.

777 Park HJ, Hong M, Bronson RT, Israel MA, Frankel WN, Yun K (2013) Elevated Id2
778 expression results in precocious neural stem cell depletion and abnormal brain
779 development. Stem Cells 31:1010–1021.

780 Paxinos G, Halliday G, Watson C, Koutcherov Y, Wang H (2007) Atlas of the developing
781 mouse brain. 1st edition. Academic Press/Elsevier, Burlington MA.

782 Przybycien-Szymanska MM, Rao YS, Prins SA, Pak TR (2014) Parental binge alcohol
783 abuse alters F1 generation hypothalamic gene expression in the absence of direct fetal
784 alcohol exposure. PLoS One 9:e89320.

Rompala GR, Finegersh A, Homanics GE (2016) Paternal preconception ethanol exposure blunts hypothalamic-pituitary-adrenal axis responsivity and stress-induced excessive fluid intake in male mice. Alcohol 53:19–25.

Rompala GR, Finegersh A, Slater M, Homanics GE (2017) Paternal preconception alcohol exposure imparts intergenerational alcohol-related behaviors to male offspring on a pure C57BL/6J background. Alcohol 60:169–177.

Rompala GR, Mounier A, Wolfe CM, Lin Q, Lefterov I, Homanics GE (2018) Heavy chronic intermittent ethanol exposure alters small noncoding RNAs in mouse sperm and epididymosomes. Front Genet 9:32.

Rompala GR, Homanics GE (2019) Intergenerational effects of alcohol: A review of paternal preconception ethanol exposure studies and epigenetic mechanisms in the male germline. Alcohol Clin Exp Res 43:1032-1045.

Rubenstein JLR, Anderson S, Shi L, Miyashita-Lin E, Bulfone A, Hevner R (1999) Genetic control of cortical regionalization and connectivity. Cereb Cortex 9:524–532.

Rustay NR, Wahlsten D, Crabbe JC (2003) Influence of task parameters on rotarod performance and sensitivity to ethanol in mice. Behav Brain Res 141:237–49.

Stockard CR, Papanicolaou GN (1918) Further studies on the modification of the germ-cells in mammals: The effect of alcohol on treated guinea pigs and their descendants. J Exp Zool 26:119-226.

Tarter RE, Jacob T, Bremer DL (1989) Specific cognitive impairment in sons of early onset alcoholics. Alcohol Clin Exp Res 13:786–789.

Thomas SE, Kelly SJ, Mattson SN, Riley EP (1998) Comparison of social abilities of children with fetal alcohol syndrome to those of children with similar IQ scores and normal controls. Alcohol Clin Exp Res 22:528–33.

809 Wolterink-Donselaar IG, Meerding JM, Fernandes C (2009) A method for gender
810 determination in newborn dark pigmented mice. Lab Anim (NY) 38:35-38.

811 Wozniak DF, Cicero TJ, Kettinger L, Meyer ER (1991) Paternal alcohol consumption in the
812 rat impairs spatial learning performance in male offspring. Psychopharmacology
813 105:289–302.

814 Xia R, Jin L, Li D, Liang H, Yang F, Chen J, Yuan W, Miao M (2018) Association between
815 paternal alcohol consumption before conception and anogenital distance of offspring.
816 Alcohol Clin Exp Res 42:735–742.

817 Yang M, Silverman JL, Crawley JN (2011). Automated three-chambered social approach
818 task for mice. Curr Protoc Neurosci 56:8.26.1-8.26-16.

819 Zhou D, Lebel C, Lepage C, Rasmussen C, Evans A, Wyper K, Pei J, Andrew G, Massey A,
820 Massey D, Beaulieu C (2011) Developmental cortical thinning in fetal alcohol spectrum
821 disorders. Neuroimage 58:16–25.

822 Zuccolo L, DeRoo LA, Wills AK, Smith GD, Suren P, Roth C, Stoltenberg C, Magnus P
823 (2017) Erratum: Pre-conception and prenatal alcohol exposure from mothers and
824 fathers drinking and head circumference: results from the Norwegian Mother-Child
825 Study (MoBa). Sci Rep 7:45877.

826

827 **FIGURE LEGENDS**

828 **Figure 1.** ***Experimental timeline.*** Mating between ethanol exposed males and ethanol
829 naive females took place following a 15-23 day 25% EtOH exposure in sires. Following
830 gestation (~20 days) 3 subsets of pups from each litter were designated for either 1)
831 sacrifice at P0 for anatomical experiments, 2) behavioral assessment at P20 or 3) weaned
832 and assessed for behavior at P30. See Table 3 for list of abbreviations.

833

Figure 2. ***Measurements of EtOH-exposed and control sires.*** **A**, Average daily liquid intake of sires (mL/day). No differences present between control (*n* = 10) and EtOH-exposed (*n* = 10) males. **B**, BEC measurements in male sires after a 20-day exposure to 25% EtOH or water (control). Sires exposed to 25% EtOH (*n* = 7) had an average BEC of 125.6 mg/dL compared to controls (*n* = 7) which had a BEC of 0 mg/dL (****$p < .0001$). See Table 3 for list of abbreviations.

Figure 3. ***P0 pup measurements.*** **A**, Brain weights at P0 in control (*n* = 14) and PatEE (*n* = 14) offspring. **B**, Cortical lengths at P0 in control (*n* = 14) and PatEE (*n* = 14) offspring. No differences are seen in P0 brain weight (**A**) or cortical length (**B**) between PatEE and controls. **C**, Litter size of control (*n* = 10) and PatEE (*n* = 10) males. See Table 3 for list of abbreviations.

Figure 4. ***Measurements of cortical anatomy in newborn (P0) mice.*** High magnification coronal sections of Nissl-stained P0 hemisections. Measurements in cortical areas included putative frontal cortex (control*: n* = 5*;* PatEE*: n* = 5) (**A1-2**), prelimbic cortex (control*: n* = 5*;* PatEE*: n* = 5) (**B1-2**), primary somatosensory cortex (control*: n* = 6*;* PatEE*: n* = 7) (**C1-2**), primary auditory cortex (control*: n* = 6*;* PatEE*: n* = 6) (**D1-2**), and primary visual cortex (control*: n* = 5; PatEE*: n* = 6) (**E1-2**). No significant differences were observed in any regions between control (**A1-E1**) and PatEE (**A2-E2**; **A3-E3**). Images oriented dorsal (D) up, lateral (L) to the right. Scale bar, 1000 μm (**A1-A2**), 500μm (**B-E**). Conventions as in previous.

Figure 5. ***Neocortical gene expression of P0 mice: Id2 and RZRβ expression in the neocortex.*** High magnification of 100 μm coronal sections following free-floating *in situ* RNA hybridization with *Id2* (control: **A1-A5**, PatEE: **B1-B5**) and *RZRβ* (control: **C1-C5**, PatEE: **D1-D5**) probes. **A2**, **A3,** section through the parietal cortex where arrows denote the lateral boundary of the most superficial layer of *Id2* expression in a control brain. **B2**, **B3**, *Id2* expression extends further laterally in PatEE brains compared to controls as seen by comparing arrow locations. Arrow in **C3**, medial boundary of *RZRβ* expression in control

parietal cortex. In PatEE brains this medial boundary for *RZRβ* has shifted medially (arrow in **D3)**. Sections oriented dorsal (D) up and lateral (L) to the right. Scale bar, 1000 μm. See Table 3 for list of abbreviations.

Figure 6. ***Analysis of gene expression.*** High magnification coronal sections of *in situ* hybridization using *RZRβ* (control: *n = 7;* PatEE: *n = 6*) (**A1-D1**) and *Id2* (control: *n = 7;* PatEE: *n* = 7) (**A2-D2**) probes in P0 cortex of control (**A1**, **A2**) and PatEE (**B1**, **B2**) mice. **C1**, **C2**, Line drawings at the cortical level where gene expression was quantified. Black boxes within the line drawings (**C1**, **C2**) indicate the ROI in which transcript densities were quantified in *RZRβ* (**D1**) and *Id2* (**D2**) sections. PatEE brains exhibited increased transcript densities in the designated ROIs for both genes compared to controls, indicating altered borders of gene expression due to PatEE. Quantified sections for both genes are at matching levels, indicating an abnormal expression phenotype that co-registered anatomically. Sections oriented dorsal (D) up and lateral (L) to the right. Scale bar, 500 μm. (**$p < 0.01$, **** $p < 0.0001$). See Table 3 for list of abbreviations.

Figure 7. ***Dye tracing of intraneocortical connections.*** Putative somatosensory and visual INC development in control (**A1-6**) and PatEE (**B1-6**) P0 brains. Rostral to caudal series of 100 μm coronal hemisections following dye placements of DiI (red) in putative somatosensory cortex (**A2**, **B2**, **asterisks**) and DiA (green) in putative visual cortex (**A5**, **B5**, **asterisks**) and dye transport. DAPI (blue) was used as counterstain. Mixed labeling of INCs is present at the somatosensory-visual boundary in PatEE (**B3-4, white arrow**) but not in controls (**A3-4**). Images oriented dorsal (D) up and lateral (L) to the right, scale bar, 1000 μm. See Table 3 for list of abbreviations.

Figure 8. ***Dye tracing quantification.*** Average visual cortex DPL spread and projection zones for P0 control (*n* = 6) and PatEE (*n* = 5) brains. **A**, Average spread of putative somatosensory cortex (S1) DPLs. PatEE brains showed no significant difference in DPL spread when compared to controls indicating consistency across cases. **B**, Average

projection zone of retrogradely labeled cells from the putative S1 DPLs. There was no significant difference in S1 DPZs of PatEE mice compared with controls. **C**, Average spread of putative visual cortex (V1) DPL. PatEE brains showed no significant difference in DPL spread when compared to controls indicating dye injection size was consistent throughout cases. **D**, Average projection zone of retrogradely labeled cells from the putative V1 DPLs. All DPL spread and projection zones are recorded as a percentage of total cortical length. See Table 3 for list of abbreviations.

Figure 9. ***Lateral cell dispersion quantification.*** Putative somatosensory and visual INC development in control (**A**) and PatEE (**B**) P0 brains at the region where mixed cell labeling and gene expression changes co-registered anatomically. **C**, Line drawing at the cortical level where cell labeling was quantified. Arrows indicate where measurements of furthest lateral labeled cells were made. **D**, Average distance from the corpus callosum of furthest laterally labeled cell from putative V1 injection. PatEE mice display increased distance of cells from the corpus callosum compared to controls. Images oriented dorsal (D) up and lateral (L) to the right, scale bar, 500 μm. See Table 3 for list of abbreviations.

Figure 10. ***Behavior at P20.*** Behavioral measures of Suok assay in age P20 mice. No significant main effects of sex or treatment were observed for falls (**A**). Missteps in female PatEE mice were significantly greater in number compared to controls; a similar result was observed in males, with a trend towards significance (**B**). Male PatEE mice crossed significantly more segments (**C**) than male controls, no differences observed in females. PatEE mice, regardless of sex, showed no significant differences compared to controls in anxiety-like behaviors as measured via rearing/grooming events (**D**), directed exploration events (**E**), and latency to leave center (**F**). (*$p < 0.05$, **$p < 0.01$). Control females ($n = 13$), control males ($n = 14$), PatEE females ($n = 16$), and PatEE males ($n = 14$). Conventions as in previous.

Figure 11. ***Behavior at P30.*** P30 behavior in PatEE and control mice as assessed by the accelerated rotarod in females (control *n* = 14, PatEE *n* = 13)(**A**) and males (control *n* = 12, PatEE *n* = 13)(**B**), forced swim test (control: female *n* = 19, male *n* = 18; PatEE: female *n* = 22, male *n* = 23)(**C**), and sociability test (control: female *n* = 15, male *n* = 12; PatEE: female *n* = 16, male *n* = 14)(**D**). **A,** No significant differences found in time spent on the rod due to treatment in females **B**, PatEE males had significantly decreased scores in trials 2 and 3 as compared to male controls. **C**, No differences in depressive-like behavior due to sex or treatment were observed as measured by the forced swim test. **D**, No significant differences were seen between control and PatEE mice, regardless of sex, in time spent with the novel mouse within the sociability test (*$p < 0.05$, ** $p < 0.01$). Conventions as in previous.

Figure 12. ***Paternal EtOH exposure model****.* Proposed model of how an EtOH-exposed sire's sperm can be negatively affected by ethanol which may lead to changes in offspring gene expression, intraneocortical connectivity, and behavior compared to the offspring of sires exposed to only water. We propose an initial epigenetic dysregulation in sperm may cause direct changes in expression patterns in genes (overlapping *RZRβ* and *Id2* patterns) who govern connectivity within the cortex, which disrupts INC patterning (overlapping mixed cells in S1 and V1 in PatEE mice) and ultimately results in abnormal later-life behavior.

Table 1. List of experimental replicates.

	Control		PatEE	
Litters	10		10	
BEC	7		7	
Cortical length	14		14	
Brain weight	14		14	
Anatomy				
FCx	5		5	
PrL	5		5	
S1	6		7	
A1	6		6	
V1	5		6	
***RZRβ* ISH**	7		6	
***Id2* ISH**	7		7	
INC tracing	6		5	
	Female	**Male**	**Female**	**Male**
Suok test	13	14	16	14
Rotarod	14	12	13	13
Forced swim test	19	18	22	23
Sociability	15	12	16	14

Table 2. Group means and SEMs for all statistical measures.

Measure (units)	**Control**	**PatEE**
Sire food intake (g/day)	7.38 ± 0.97	5.49 ± 0.64, *9*
Sire liquid intake (mL/day)	9.775 ± 0.470	9.928 ± 0.888
Sire BEC (mg/dL)	0.0 ± 0.0	125.6 ± 10.50
Sire weight gain (g)	0.67 ± 0.9	0.20 ± 0.8
Litter size (# of pups)	12.40 ± 1.147	11.30 ± 1.174
P0 brain weight (g)	0.1055 ± 0.005	0.1002 ± 0.003
P0 cortical length (mm)	4.870 ± 0.072	4.885 ± 0.060
FCx cortical thickness (% change)	100.0 ± 2.608	99.49 ± 2.973
PrL cortical thickness (% change)	100.0 ± 3.378	102.3 ± 3.838
S1 cortical thickness (% change)	100.0 ± 2.984	107.6 ± 3.964
A1 cortical thickness (% change)	100.0 ± 5.814	110.1 ± 3.395
V1 cortical thickness (% change)	100.0 ± 4.607	99.32 ± 2.220
RZRβ transcript density (% area fraction)	6.475 ± 0.678	17.21 ± 4.55
Id2 transcript density (% area fraction)	6.849 ± 3.422	48.503 ± 6.151
Putative S1 DPL spread (% total cortical length)	14.94 ± 0.93	15.35 ± 1.072
Putative V1 DPL spread (% total cortical length)	13.86 ± 0.57	12.65 ± 0.46
SCx Dye projection zone (% total cortical length)	45.17 ± 2.842	49.96 ± 3.183
VCx Dye projection zone (% total cortical length)	38.78 ± 2.16	48.12 ± 3.83
V1 Lateral cortical cell dispersion (μm)	1081 ± 158.5	1524 ± 96.28
Suok- Missteps (# of events)	Female: 3.538 ± 0.81 Male: 3.500 ± 0.52	Female: 14.00 ± 2.50 Male: 11.36 ± 3.09
Suok- Falls (# of events)	Female: 0.923 ± 0.38 Male:1.214 ± 0.32	Female: 2.250 ± 0.62 Male: 2.571 ± 0.82
Suok- Segments crossed (# of events)	Female: 119.4 ± 14.79 Male: 97.00 ± 15.76	Female: 159.4 ± 10.23 Male: 165.4 ± 17.68
Suok- Rearing/grooming (# of events)	Female: 1.00 ± 0.28 Male: 1.357 ± 0.23	Female: 0.57 ± 0.20 Male: 1.00 ± 0.60

Suok- Latency to leave center (s)	Female: 3.15 ± 0.47 Male: 4.03 ± 0.88	Female: 2.25 ± 0.37 Male: 3.57 ± 0.83
Suok- Directed exploration (# of events)	Female: 62.92 ± 9.7 Male: 60.14 ± 11.56	Female: 86.81 ± 7.64 Male: 77.23 ± 6.74
AR trial 1 (s)	Female: 194.43 ± 30.2 Male: 156.91 ± 22.9	Female: 214.62 ± 26.3 Male: 114.85 ± 26.7
AR trial 2 (s)	Female: 277.64 ± 10.5 Male: 275.5 ± 13.1	Female: 241.00 ± 24.6 Male: 178.5 ± 27.7
AR trial 3 (s)	Female: 290.43 ± 5.4 Male: 289.1 ± 6.2	Female: 254.69 ± 20.6 Male: 210.3 ± 28.6
AR trial 4 (s)	Female: 271.14 ± 13.3 Male: 283.00 ± 12.4	Female: 291.92 ± 5.3 Male: 258.46 ± 22.4
FST time immobile (s)	Female: 154.6 ± 12.06 Male: 142.4 ± 18.50	Female: 122.1 ± 15.28 Male: 103.9 ± 16.00
Sociability time with mouse (s)	Female: 257.7 ± 15.97 Male: 256.9 ± 18.67	Female: 248.8 ± 16.00 Male: 307.8 ± 20.73

Table 3. List of abbreviations used.

Abbreviation	Name
EtOH	Ethanol
PatEE	Paternal ethanol exposure
FASD	Fetal alcohol spectrum disorders
P	Postnatal day
INCs	Intraneocortical connections
BEC	Blood ethanol concentration
FCx	Frontal cortex
PrL	Prelimbic cortex
S1	Primary Somatosensory cortex
A1	Primary Auditory cortex
V1	Primary Visual cortex
ISH	*In situ* hybridization
***RZR*β**	Retinoid Z receptor beta
Id2	Inhibitor of DNA binding 2
ROI	Region of interest
DPL	Dye placement location
DPZ	Dye projection zone
AR	Accelerated rotarod
FST	Forced swim test
PrEE	Prenatal ethanol exposure
CTX	Cortex
CC	Corpus callosum
LV	Lateral ventricle
CPu	Caudate putamen
snRNA	Small non-coding RNA

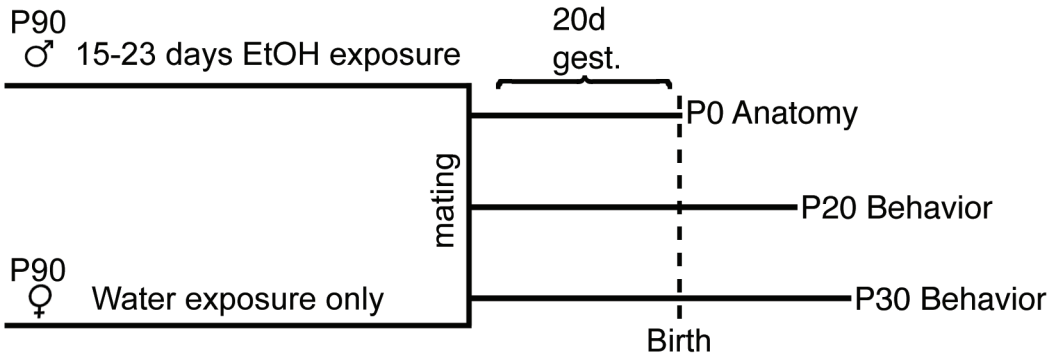

acer_14245_f1.tif

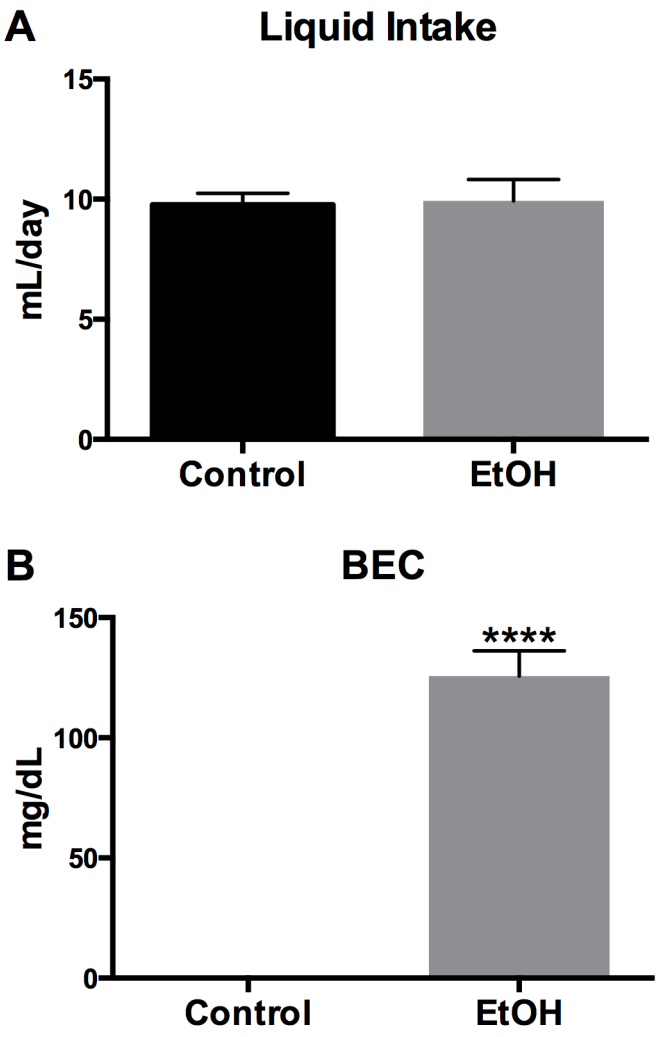

acer_14245_f2.tiff

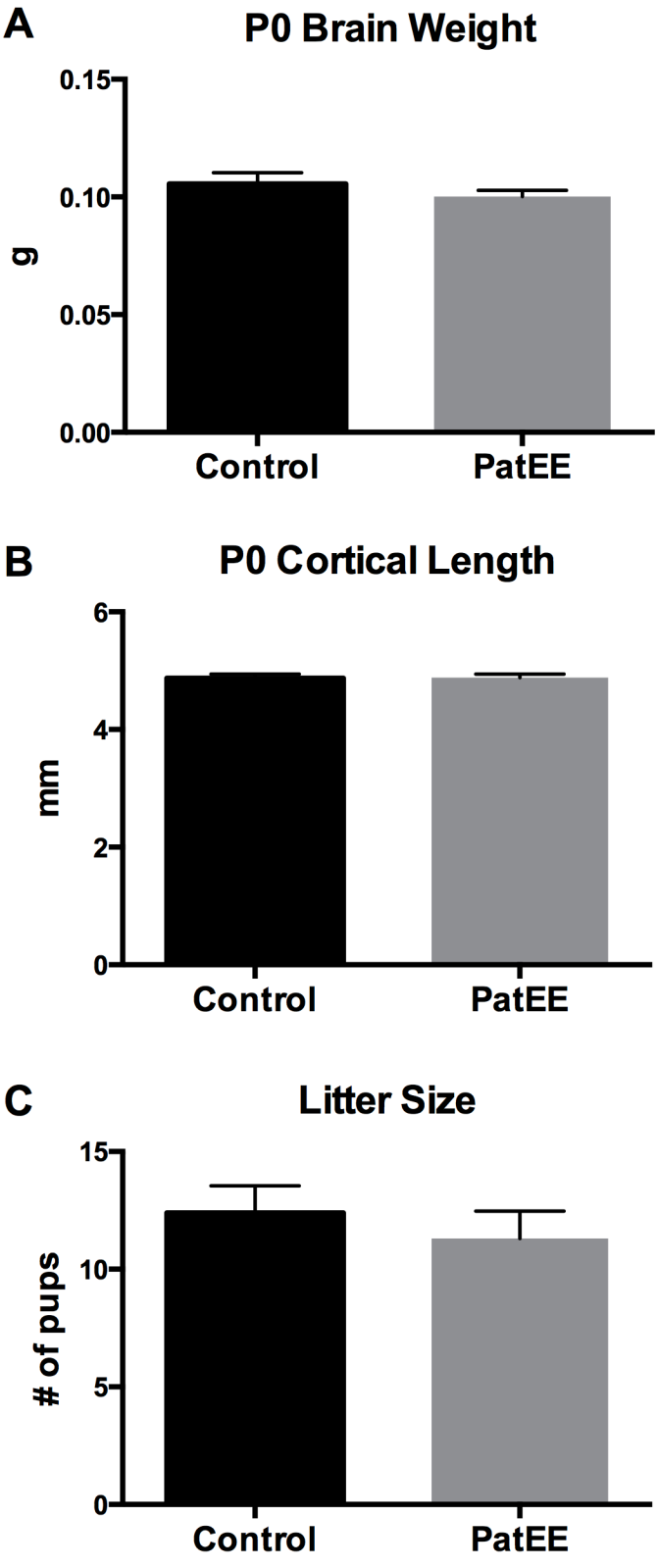

acer_14245_f3.tiff

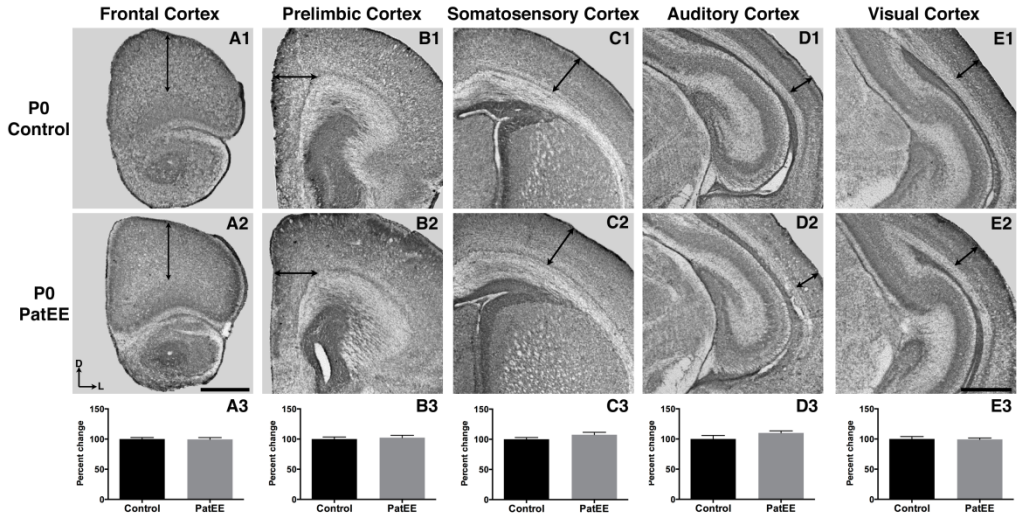

acer_14245_f4.tif

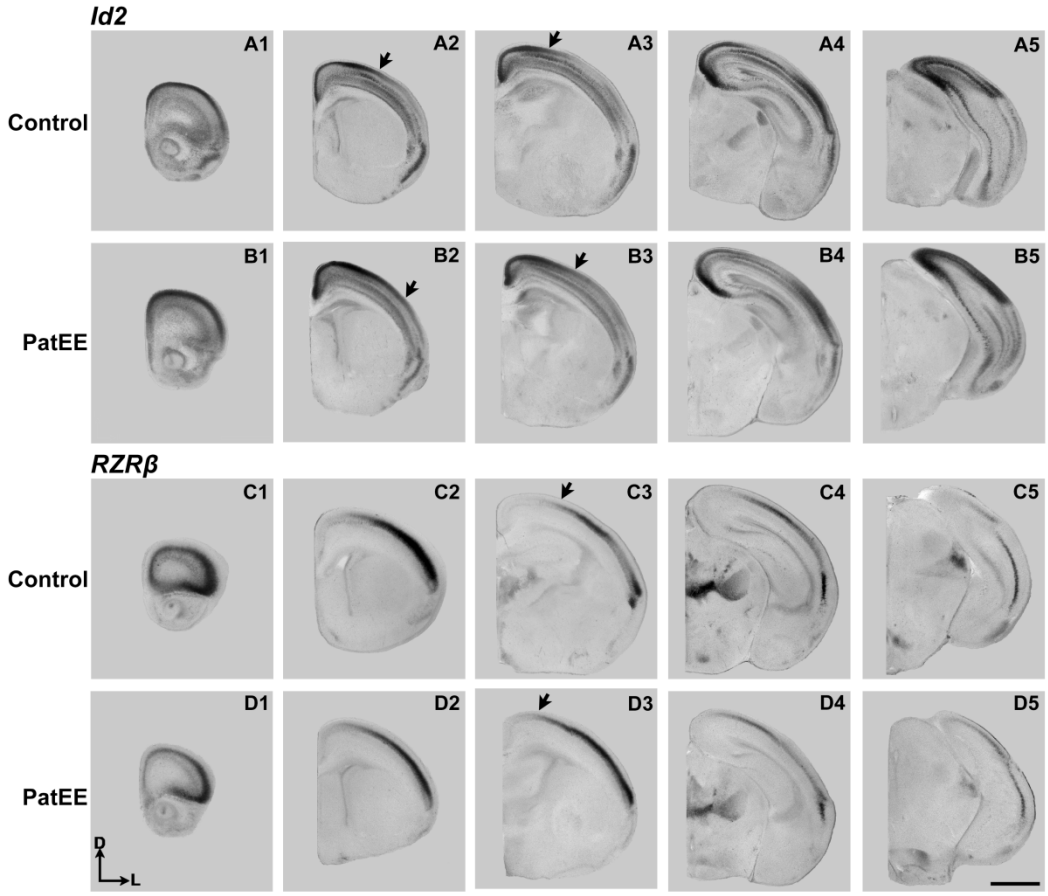

acer_14245_f5.tif

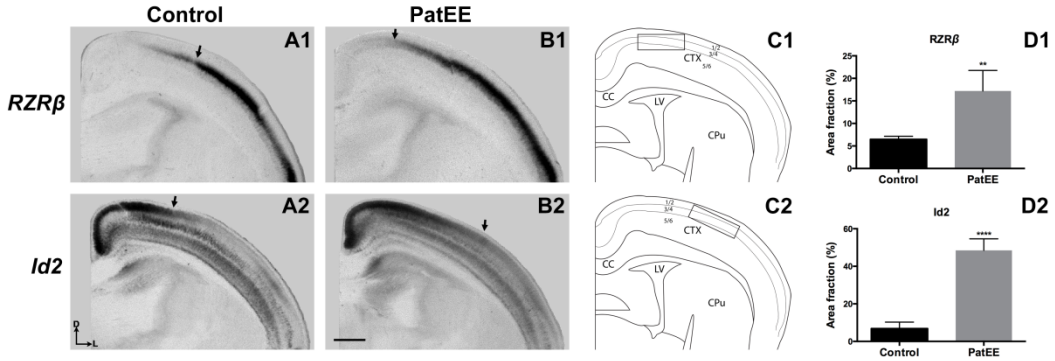

acer_14245_f6.tif

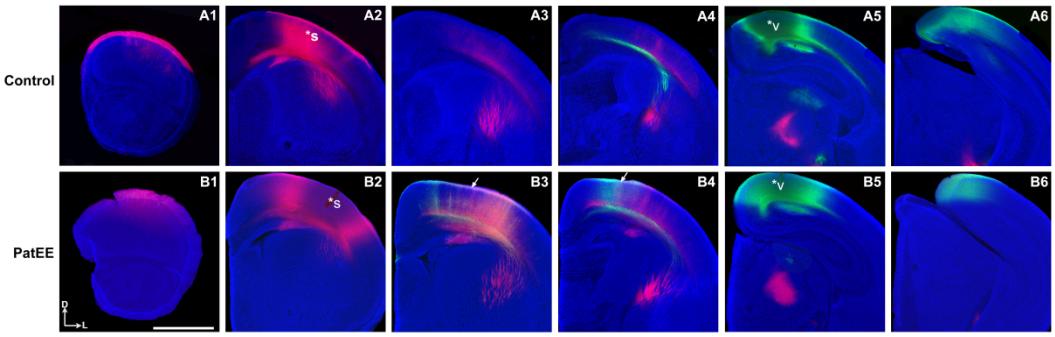

acer_14245_f7.tif

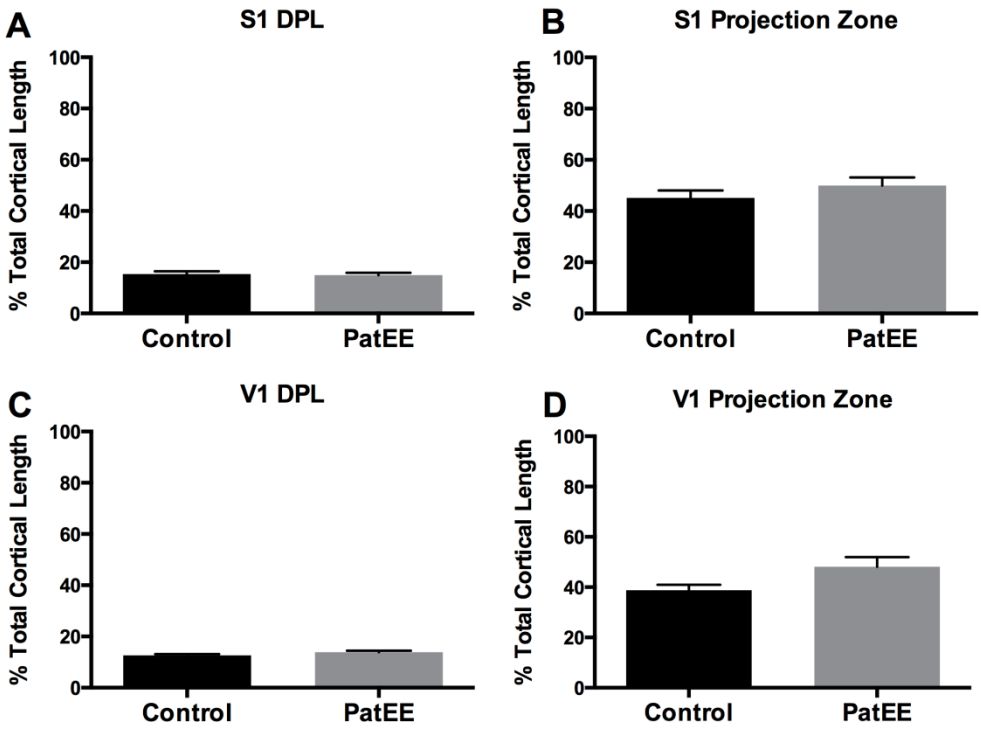

acer_14245_f8.tiff

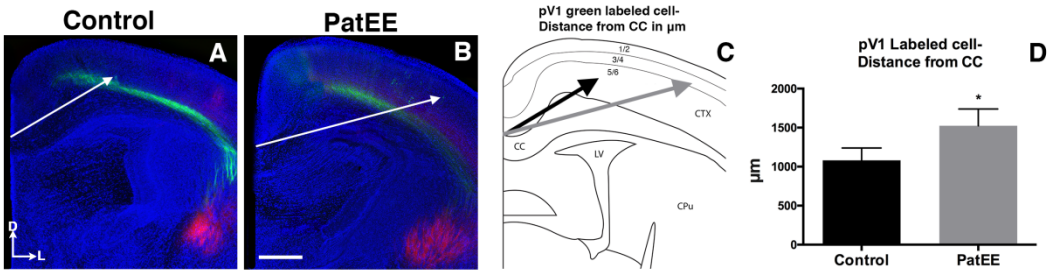

acer_14245_f9.tif

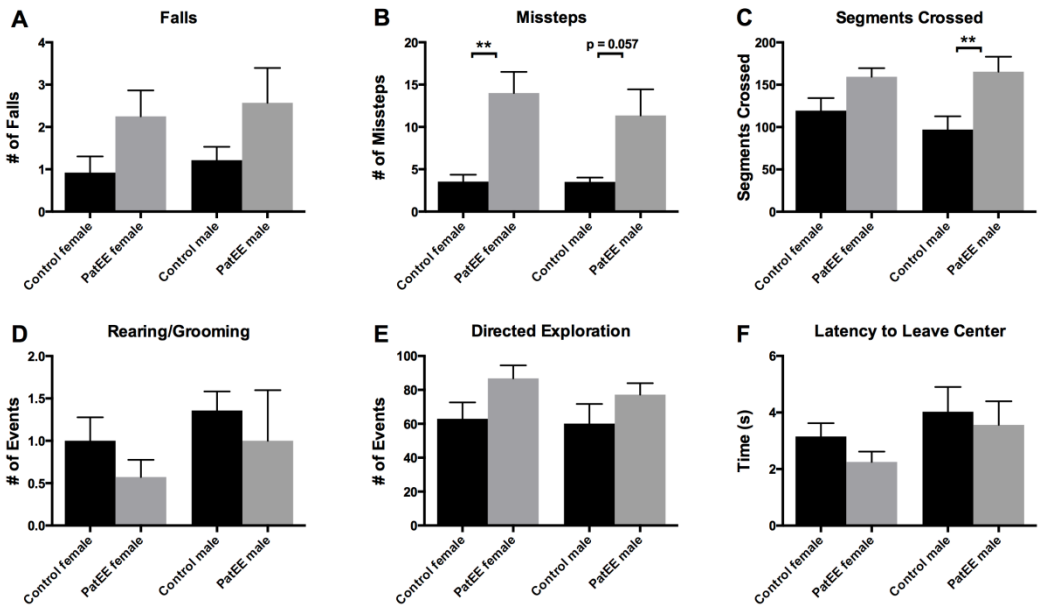

acer_14245_f10.tiff

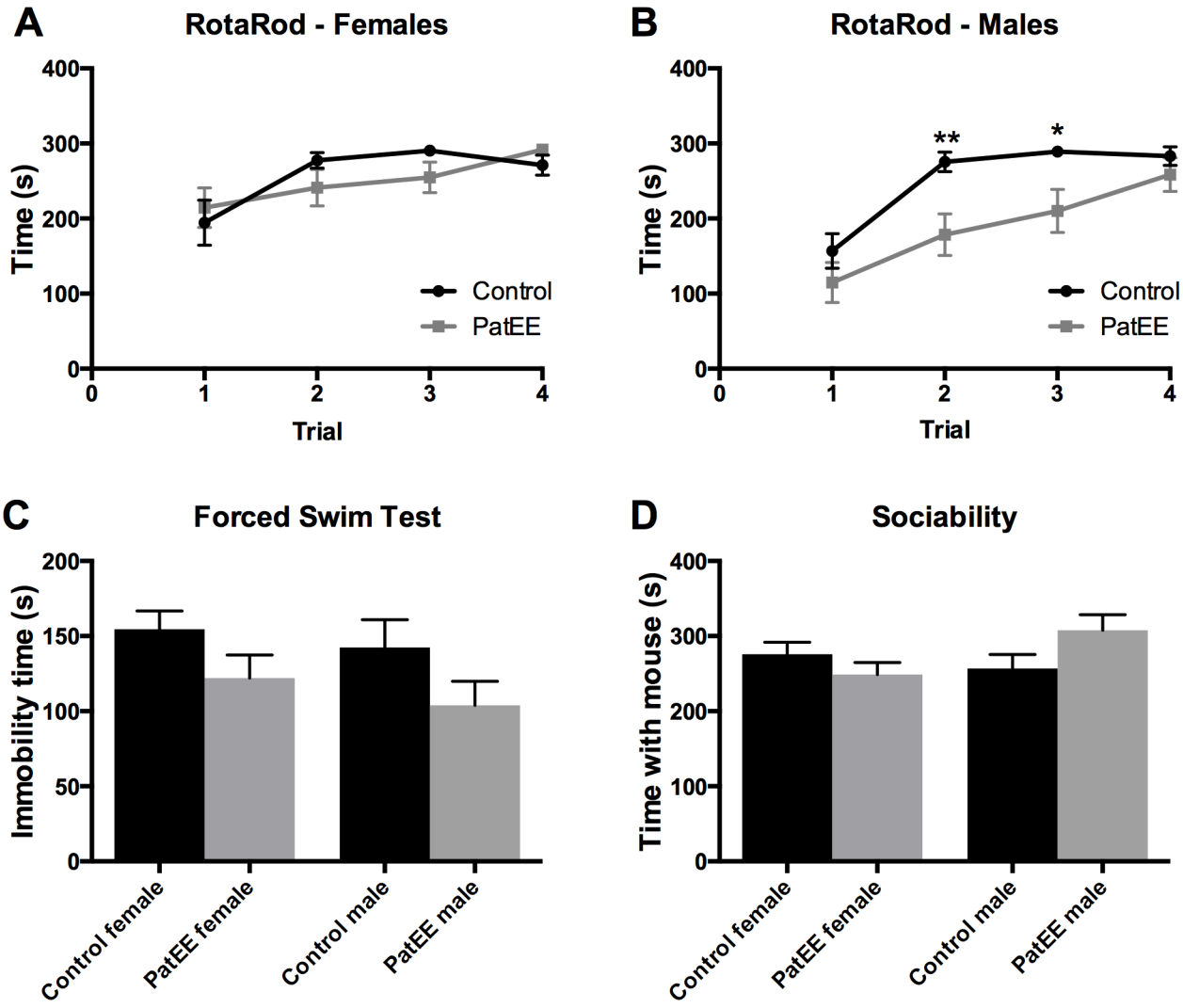

acer_14245_f11.tiff

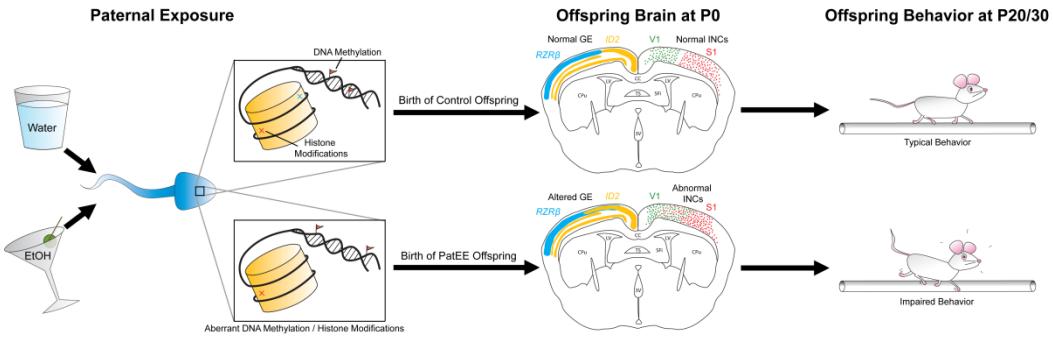

acer_14245_f12.tif